

APPENDIX C2: Design of Canard Aircraft

This appendix is a part of the book **General Aviation Aircraft Design: Applied Methods and Procedures** by Snorri Gudmundsson, published by Elsevier, Inc. The book is available through various bookstores and online retailers, such as www.elsevier.com, www.amazon.com, and many others.

The purpose of the appendices denoted by C1 through C5 is to provide additional information on the design of selected aircraft configurations, beyond what is possible in the main part of **Chapter 4, Aircraft Conceptual Layout**. Some of the information is intended for the novice engineer, but other is advanced and well beyond what is possible to present in undergraduate design classes. This way, the appendices can serve as a refresher material for the experienced aircraft designer, while introducing new material to the student. Additionally, many helpful design philosophies are presented in the text. Since this appendix is offered online rather than in the actual book, it is possible to revise it regularly and both add to the information and new types of aircraft. The following appendices are offered:

- C1 – Design of Conventional Aircraft
- C2 – Design of Canard Aircraft (this appendix)
- C3 – Design of Seaplanes
- C4 – Design of Sailplanes
- C5 – Design of Unusual Configurations

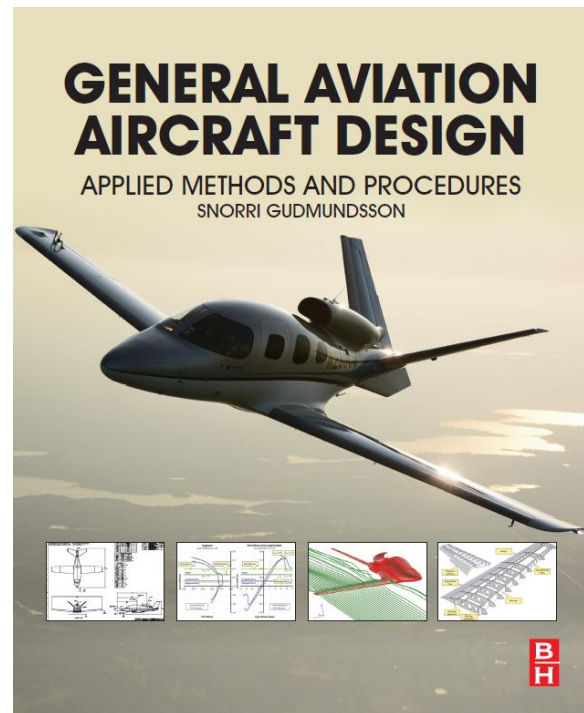


Figure C2-1: A single engine, four-seat Velocity 173 SE just before touch-down. (Photo by Phil Rademacher)

C2.1 Design of Canard Configurations

It has already been stated that preference explains why some aircraft designers (and manufacturers) choose to develop a particular configuration. In other situations such partiality is absent and the selection of the configuration actually presents an organizational conflict. However, while the selection of a particular tail configuration (e.g. conventional, T-tail, etc.) may pose a challenge, whether to place the horizontal tail in front of or aft of the wing is usually not up for debate. In either case, the location of the horizontal tail is indeed of primary importance and this calls for a deep understanding of the implications of its selection. Most frequently, the configuration options consist of a conventional tail-aft, canard, or a three-surface configuration. Figure C2-2 shows the layout of a typical canard aircraft. The configuration is unique in appearance and offers some good properties. This appendix discusses various issues that must be kept in mind when designing a canard aircraft. The canard configuration was discussed in some detail in [Section 11.3.12, Canard Configuration](#). This section picks up where that discussion left off.

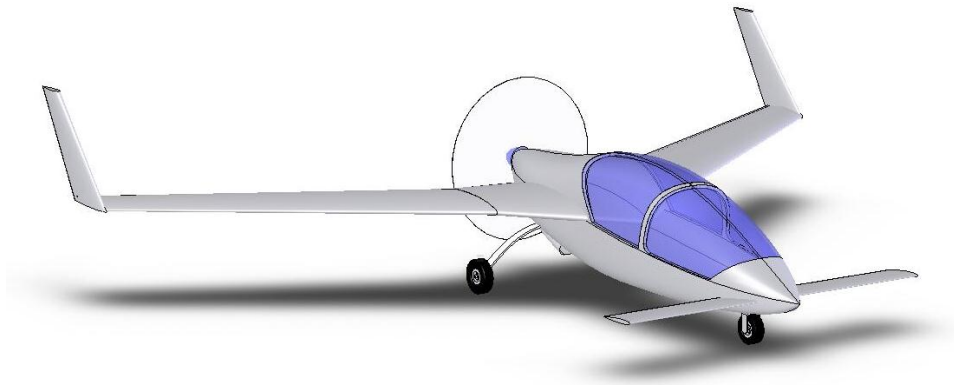


Figure C2-2: A small canard configuration.

C2.1.1 Pros and Cons of the Canard Configuration

The first question to consider regarding the canard configuration has to do with stability and control. A horizontal lifting surface placed forward of the main wing results in a destabilizing pitching moment, which would render the vehicle unstable were it not for the forward placement of the CG. In fact, the CG must be placed far forward of the aerodynamic center of the Mean Geometric Chord in order to produce a stabilizing moment. This renders the aircraft stable, in other words, yields a $C_{m\alpha} < 0$. The challenge for the designer is to determine the geometry of the canard, which includes an airfoil selection, such that two conditions are satisfied: (1) the $C_{m\alpha}$ is indeed negative and (2) C_{m0} is greater than zero. The former is controlled using the CG location and the latter using geometry, canard incidence angle, and airfoil selection.

While downwash generally reduces the stability of a tail-aft aircraft (as it results in a nose-up pitching moment), it allows the HT to be installed at a much smaller Angle-of-Incidence (AOI) than possible with a canard (assuming symmetrical airfoils – cambered airfoils will be discussed later). Consider a canard featuring a symmetrical airfoil (i.e. $C_{i0} = 0$). In order to satisfy condition (2) above (i.e. $C_{m0} > 0$) this airfoil would require a large AOI (or TED elevator deflection) to allow the aircraft to be trimmed at an AOA that generates positive C_L . One of the reasons for this is the limited upwash in front of the main wing. This would hold even at modest Static Margin. This predicament is generally solved by selecting a highly cambered airfoil (which has $C_{i0} \gg 0$) and high AR planform shape (whose $C_{L\alpha} \gg 0$).

Figure C2-3 highlights the difference in the location of the stick-fixed neutral points of a conventional tail-aft and a canard aircraft. Each configuration has two icons that represent the stick-fixed neutral point and CG location that

yields a 0.10 Static Margin. Note that adding a fuselage would destabilize both configurations and push all points (neutral and, thus, the CG) forward.

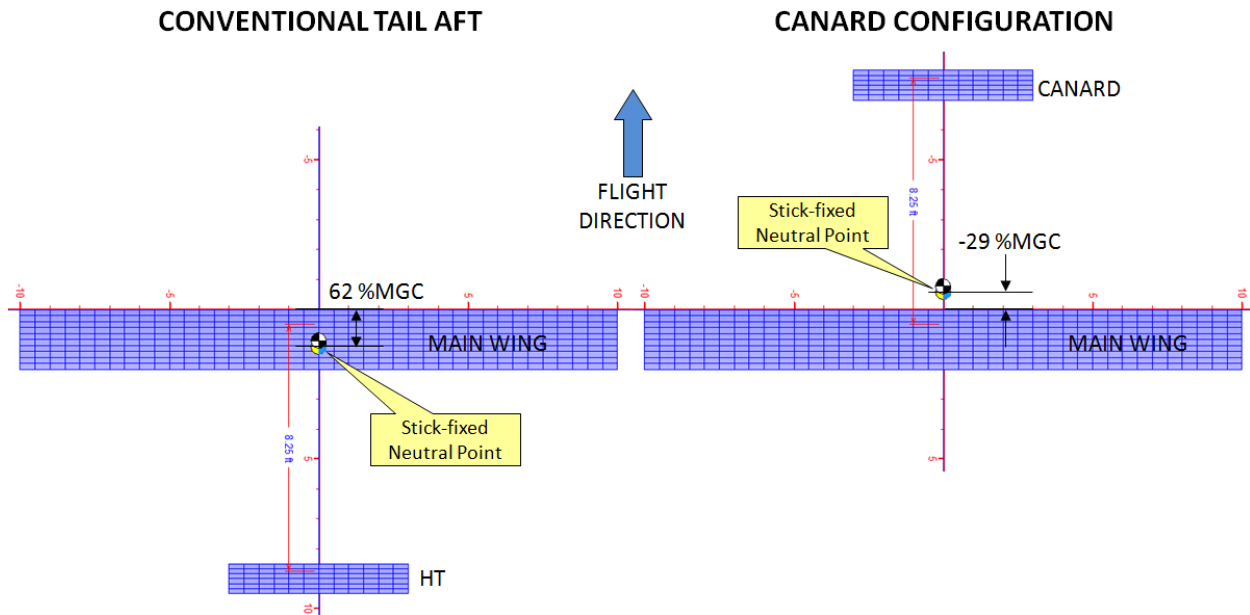


Figure C2-3: Comparing the stick-fixed neutral points and CG locations required for a Static Margin of 0.10 of a conventional tail aft (left) and canard (right) configurations. The neutral points were determined using potential flow theory. Note the numbers only apply to this specific geometry.

Finally, since the CG is in front of the wing, moving it farther forward both shortens the balancing tail arm and increases the wing arm. Since the wing lift force is much greater than that of the canard, the CG cannot move too far forward before an uncontrollable nose-pitch down moment is generated. This limits the practical CG envelope of the configuration. For instance, the twin engine Beech Starship required a swing-wing style canard to increase its nose pitch-up authority when deploying flaps. Another issue is that the chord length of the canard is usually small enough to be subject to Reynolds number effects. One of the consequences can be a diminished pitch authority at low airspeeds, when the small-chord airfoil is subject to early flow separation that reduces its lift curve slope. This can also lead to noticeable longitudinal trim changes when flying in precipitation, as is reflected in a caution, placarded in the Pilot's Operating Handbook for the Rutan Long-EZ¹. The caution states that when entering visible precipitation, the Long-EZ may experience a significant pitch trim change, as experienced in the Long-EZ prototype (N79RA). It goes on to state that owners of Rutan's earlier canard aircraft, report either nose up or nose down pitch changes. Builders are warned that each aircraft may react differently. It is recommended that airspeed above 90 knots be maintained in rain as this allows the aircraft to be trimmed with hands off the control stick.

In spite of these shortcomings, many existing canard aircraft are well designed in the view of this author, including the Rutan LongEz, and the AASI Jetcruzer, the first aircraft to have been certified in the US under 14 CFR Part 23 as "spin-resistant."

C2.1.2 Modeling the Pitching Moment for a Simple Wing-Canard System

Figure C2-4 shows a simple Wing-Canard system, intended to derive a few longitudinal static stability methods that are helpful when sizing a canard configuration aircraft. The longitudinal static stability of the configuration can be represented using Equation (11-10), repeated here for convenience:

$$C_m = C_{m_0} + C_{m_\alpha} \cdot \alpha + C_{m_{\delta_e}} \cdot \delta_e \quad (C2-1)$$

Where:

- C_{m_0} = Coefficient of moment at zero AOA
- C_{m_α} = Change in coefficient of pitching moment due to AOA
- $C_{m_{\delta_e}}$ = Elevator authority; change in coefficient of pitching moment due to elevator deflection

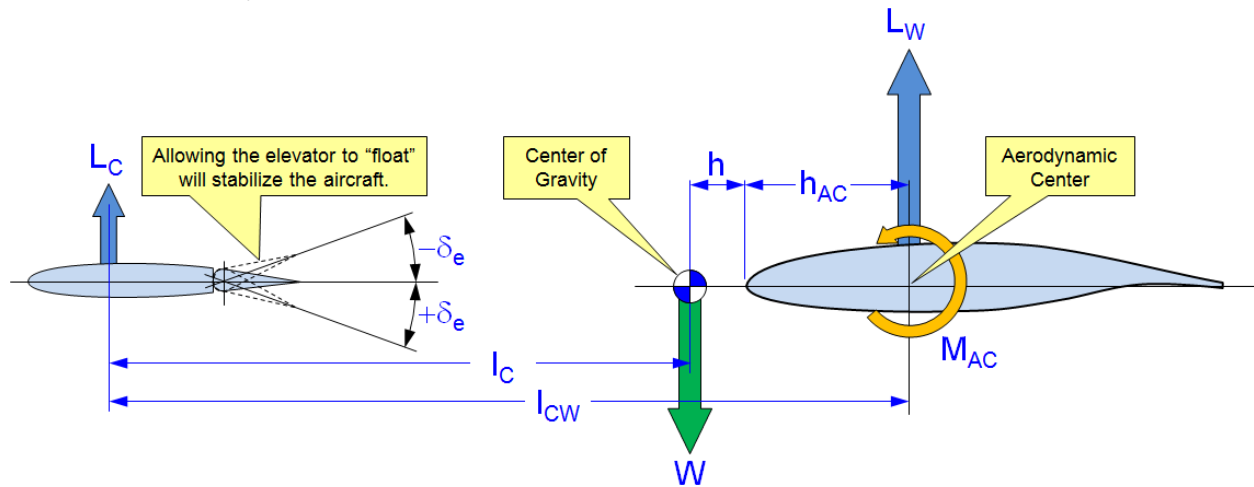


Figure C2-4: Wing-Canard system used to derive Equation (C2-4).

Both of the above terms can be determined for this system using the following expressions:

$$C_{m_0} = V_C \cdot C_{L_{0C}} + C_{m_{0AC}} - C_{m_{0W}} \quad (C2-2)$$

$$C_{m_\alpha} = V_C \cdot C_{L_{\alpha C}} + C_{m_{\alpha AC}} - \frac{(h_{AC} + h)}{C_{MGC}} C_{L_{\alpha W}} \quad (C2-3)$$

Where:

- C_{MGC} = Mean Geometric Chord
- h_n = Physical location of the CG at which $C_{m_\alpha} = 0$; i.e. the stick-fixed neutral point
- h_{AC} = Physical location of the Aerodynamic Center
- l_C = Arm between the aerodynamic center of the canard and CG
- l_{CW} = Arm between the aerodynamic center of the canard and the wing
- S = Reference wing area
- S_C = Planform area of the canard
- $V_C = \text{Canard volume} = \frac{S_C \cdot l_C}{S \cdot C_{MGC}} = \frac{S_C \cdot (l_{CW} - h - h_{AC})}{S \cdot C_{MGC}}$
- $C_{m_{0AC}}$ = Longitudinal stability contribution of components other than the wing
- $C_{m_{0W}} = C_{L_0} (h_{AC} + h)$ = Wing pitching moment due to airfoil camber
- $C_{L_{0C}}$ = Canard lift coefficient at zero AOA
- $C_{m_{\alpha AC}}$ = Longitudinal stability contribution of components other than the wing
- $C_{L_{\alpha C}}$ = Lift curve slope of the canard
- $C_{L_{\alpha W}}$ = Wing lift curve slope

Note that the term $C_{m_{\alpha AC}}$ refers to the stabilizing effects of components such as the fuselage, nacelles, landing gear, the wing itself, and so on, as a function of the AOA. If the sum of these moments acts to rotate the LE down, then $M_{AC} < 0$ (has a negative sign and is stabilizing). If it acts to rotate LE up, then $M_{AC} > 0$ (has a positive sign and is destabilizing). The sign ultimately depends on the aircraft configuration. Note that the destabilizing effects of fuselages and nacelles can be estimated using the so-called Munk-Multhopp method, which is presented in [Appendix C1.6, Additional Tools for Tail Sizing](#).

DERIVATION:

It is imperative to keep the orientation of the M_{AC} in mind for the following derivation. Also note that the subscript “C” refers to the canard, but it contrasts “HT” in the derivation for [Equation \(11-26\)](#). Also, by default, it is assumed that the elevator deflection is neutral, i.e. $\delta_e = 0^\circ$.

First, determine the sum of moments about the CG. For static stability, this must equal zero. Taking nose down moments to be negative and treating all distances as having a positive value (although if the CG in Figure C2-4 is to the right of the LE, then $h < 0$), this requires:

$$\sum M_{CG} = 0 \Rightarrow -L_W(h_{AC} + h) + L_C \cdot l_C + M_{AC} = 0 \quad (i)$$

Note that the sign for M_{AC} here is “+”. Therefore, if M_{AC} is stabilizing ($M_{AC} < 0$) we will get $+(-|M_{AC}|) = -M_{AC}$, where $|\cdot|$ stands for the absolute value.

The definitions of wing lift is $L_W = q \cdot S \cdot C_{L_W}$, the lift of the canard is $L_C = q \cdot S_C \cdot C_{L_C}$, and additional moments, $M_{AC} = q \cdot S \cdot C_{MGC} \cdot C_{m_{AC}}$. Insert these into Equation (i) and divide through by $q \cdot S \cdot C_{MGC}$ as shown below:

$$\begin{aligned} -q \cdot S \cdot C_{L_W}(h_{AC} + h) + q \cdot S_C \cdot C_{L_C} \cdot l_C + q \cdot S \cdot C_{MGC} \cdot C_{m_{AC}} &= 0 \\ \Rightarrow -\frac{(h_{AC} + h)}{C_{MGC}} C_{L_W} + \underbrace{\frac{S_C \cdot l_C}{S \cdot C_{MGC}}}_{\equiv V_C} \cdot C_{L_C} + C_{m_{AC}} &= 0 \end{aligned}$$

Where V_C is the *canard volume*. Note that it depends on the CG location through l_C . This can also be represented in terms of the fixed distance between the two lifting surfaces, l_{CW} , as shown in the text above. Next, insert the definitions for C_{L_W} and C_{L_C} :

$$-\frac{(h_{AC} + h)}{C_{MGC}} (C_{L_{0W}} + C_{L_{\alpha W}} \alpha) + V_C \cdot (C_{L_{0C}} + C_{L_{\alpha C}} \alpha_C) + C_{m_{AC}} = 0 \quad (ii)$$

Note that unlike the derivation for [Equation \(11-26\)](#), the canard will not be presumed to feature a symmetrical airfoil. This is necessitated by the fact that canards typically feature highly cambered airfoils to ensure the zero-alpha lift coefficient is not zero; i.e. $C_{L_{0C}} \neq 0$. Also note that since the canard sits in the wing upwash, its AOA is increased slightly. However, this effect can be ignored if the canard is relatively far ahead of the wing, as is usually the case. Therefore, it is assumed that the AOA of the canard is equal to that of the wing. In other words: $\alpha_C = \alpha$.

Next, expand Equation (ii):

$$-\frac{(h_{AC} + h)}{C_{MGC}} C_{L_{0W}} - \frac{(h_{AC} + h)}{C_{MGC}} C_{L_{\alpha W}} \alpha + V_C \cdot C_{L_{0C}} + V_C \cdot C_{L_{\alpha C}} \alpha + C_{m_{AC}} = 0$$

Let $C_{m_{0W}} = \frac{(h_{AC} + h)}{C_{MGC}} C_{L_{0W}}$ and recall that $C_{m_{AC}} = C_{m_{0AC}} + C_{m_{\alpha AC}} \cdot \alpha$. Insert these and simplify by gathering contributions that do and do not change with the AOA:

$$\underbrace{V_C \cdot C_{L_{0C}} + C_{m_{0AC}} - C_{m_{0W}}}_{\text{Contribution that does not change with AOA}} + \underbrace{\left[V_C \cdot C_{L_{\alpha C}} + C_{m_{\alpha AC}} - \frac{(h_{AC} + h)}{C_{MGC}} C_{L_{\alpha W}} \right]}_{\text{Contribution that changes with AOA}} \alpha = 0$$

The contribution that does not change with AOA (constant terms) are typically denoted by C_{m_0} , whereas contribution that changes with AOA is denoted by C_{m_α} . This convention is maintained here as well.

QED

EXAMPLE C2-1:

Estimate the C_{m_0} and C_{m_α} for the canard configuration in Figure C2-3 and plot for AOAs ranging from -5° to 20° , using the following data. Note the Angle-of-Incidence (AOI) for the wing and canard.

MAIN WING

$$C_{MGC} = 2.0 \text{ ft}$$

$$b = 20.0 \text{ ft}$$

$$S = 40 \text{ ft}^2$$

$$C_{L_{0W}} = 0.35$$

$$C_{L_{\alpha W}} = 5.012 \text{ per radian}$$

$$\text{AOI} = 0^\circ$$

CANARD

$$C_c = 1.0 \text{ ft}$$

$$b_c = 6.0 \text{ ft}$$

$$S_c = 6.0 \text{ ft}^2$$

$$C_{L_{0C}} = 0.0 \text{ (symmetrical airfoil)}$$

$$C_{L_{\alpha C}} = 4.247 \text{ per radian}$$

$$\text{AOI}_c = 0^\circ$$

OTHER

$$h_{AC} = 0.25 \cdot C_{MGC} = 0.5 \text{ ft}$$

$$h = 0.783 \text{ ft (ahead of wing LE)}$$

$$l_c = 8.25 - h - h_{AC} = 6.967 \text{ ft}$$

$$C_{m_{0AC}} = 0$$

$$C_{m_{\alpha AC}} = 0$$

Assume the wing airfoil is NACA 4415, which was also the subject of [Example 11-1](#), and that the canard has a symmetrical airfoil. Note that the lift curve slopes were calculated using [Equation \(9-57\)](#). Assume that the 3-dimensional $C_{L_{0W}}$ is the same as that of the airfoil.

SOLUTION:

Begin by calculating the canard volume:
$$V_C = \frac{S_c \cdot l_c}{S \cdot C_{MGC}} = \frac{6.0 \times 6.967}{40 \times 2.0} = 0.5225$$

C_{l_α} for the NACA 4415 from [Table 8-5](#) is 0.106 per degree or 6.073 per radian. C_{l_α} for a typical symmetrical airfoil is 0.100 per degree or 5.730 per radian. Assuming low subsonic airspeed ($M \approx 0$) and using [Equation \(9-57\)](#) to estimate the 3D lift curve slope of the wing ($AR = 10$) and canard ($AR_c = 6$), yields a $C_{L_{\alpha W}} = 5.012$ and

$C_{L_{\alpha C}} = 4.247$, respectively. The $C_{L_{0W}}$ can be estimated using [Equation \(9-61\)](#) and data from [Table 8-5](#), where

the $\alpha_{zL} = -4^\circ$ for the NACA 4415 airfoil. Therefore,
$$C_{L_{0W}} = |\alpha_{zL}| C_{L_{\alpha W}} = \left| -4 \times \frac{\pi}{180} \right| (5.012) = 0.350.$$

Then calculate
$$C_{m_{0W}} = \frac{(h_{AC} + h)}{C_{MGC}} C_{L_{0W}} = \frac{(0.5 + 0.783)}{2.0} 0.35 = 0.2245$$

By plugging and chugging Equations (C2-2) and (C2-3) we get:

$$C_{m_0} = V_C \cdot C_{L_{0C}} + C_{m_{0AC}} - C_{m_{0W}} = 0.5225 \cdot 0 + 0 - 0.2245 = -0.2245$$

$$C_{m_\alpha} = V_C \cdot C_{L_{\alpha C}} + C_{m_{\alpha AC}} - \frac{(h_{AC} + h)}{C_{MGC}} C_{L_{\alpha W}}$$

$$= 0.5225 \times 4.247 + 0 - \frac{(0.5 + 0.783)}{2.0} (5.012) = -0.9961 \text{ per radian}$$

The resulting graph can be seen in Figure C2-5. It shows that the above prediction places the pitching moment curve below the horizontal axis for AOAs > 0. This means that in this configuration (i.e. featuring a symmetrical canard airfoil at an AOI = 0°), the airplane cannot be trimmed at an AOA that generates a positive lift coefficient. To fix this, an additional positive pitching moment must be generated. For instance, if we wanted to trim the aircraft at an AOA of 10°, the C_{m_0} must be shifted up by a magnitude of 0.398, or to $C_{m_0} = +0.174$. This additional moment is typically provided by playing with the variables of Equation (C2-2). This is discussed further in [Section C2.1.4, Requirements for the Trimmability of the Canard](#).

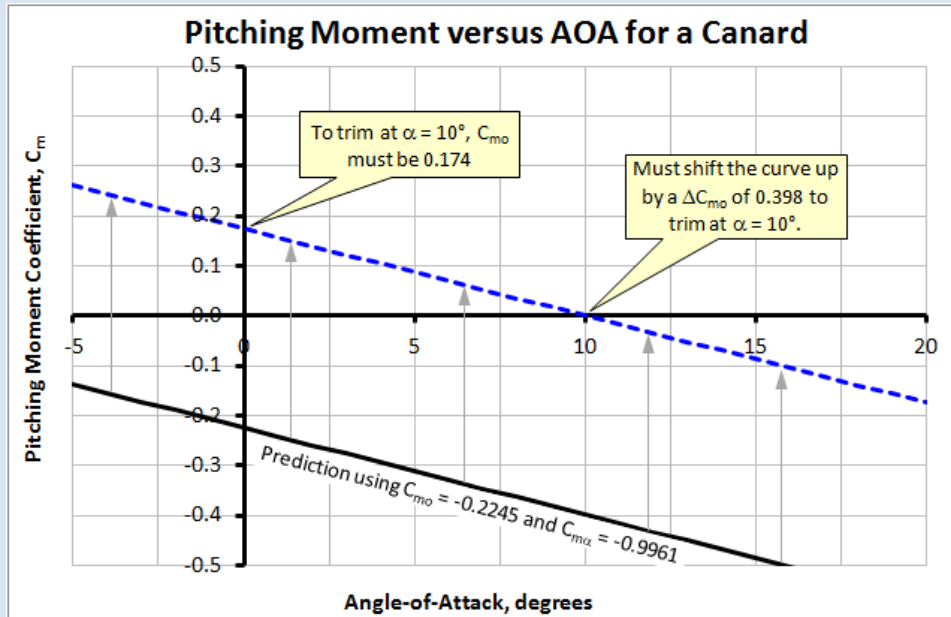


Figure C2-5: The pitching moment coefficient calculated for the arbitrary value of $h = 0.783$ ft (solid curve). The dashed curve represents how the solid curve must be shifted to allow the vehicle to be trimmed at a 10° . The upward shift can be accomplished by deflecting the elevator TED or using a cambered airfoil (or a combination thereof).

C2.1.3 The Stick-Fixed and Stick-Free Neutral Points of a Canard Configuration

Similar to [Equation \(11-26\)](#) of [Section 11.2.6, The Stick-Fixed and Stick-Free Neutral Points](#), the stick-fixed neutral point for a canard configuration can be obtained from Equation (C2-3) when the slope of the moment curve becomes zero, i.e. $C_{m_\alpha} = 0$:

$$\frac{h_n}{C_{MGC}} = \frac{\frac{(l_{CW} - h_{AC})}{C_{MGC}} S_C \cdot C_{L_{\alpha C}} + S \cdot \left(C_{m_{\alpha AC}} - \frac{h_{AC}}{C_{MGC}} C_{L_{\alpha W}} \right)}{S \cdot C_{L_{\alpha W}} + S_C \cdot C_{L_{\alpha C}}} \quad (C2-4)$$

Note that Equation (C2-4) returns a value that is measured from the leading edge of the MGC forward toward the canard (as shown in Figure C2-4). See [Example C2-2](#) for more details. Refer to Figure C2-4 for physical dimensions.

DERIVATION:

Equation (C2-3), repeated below for convenience, is the slope of the pitching moment curve:

$$C_{m_{\alpha}} = V_C \cdot C_{L_{\alpha C}} + C_{m_{\alpha AC}} - \frac{(h_{AC} + h)}{C_{MGC}} C_{L_{\alpha W}} \quad (C2-3)$$

Note that V_C is a function of h , where the distance between the two lifting surfaces at all times is constant, l_{CW} , as shown in Figure C2-4, and is given by:

$$l_{CW} = l_C + h + h_{AC} \Leftrightarrow l_C = l_{CW} - h - h_{AC} \quad (i)$$

The neutral point, by definition, occurs when $C_{m_{\alpha}} = 0$, i.e.:

$$\frac{S_C \cdot (l_{CW} - h - h_{AC})}{S \cdot C_{MGC}} \cdot C_{L_{\alpha C}} + C_{m_{\alpha AC}} - \frac{(h_{AC} + h)}{C_{MGC}} C_{L_{\alpha W}} = 0 \quad (ii)$$

This depends primarily on the location of the CG, denoted by h . By renaming the CG location as h_n and expanding Equation (ii) and dividing through by the lift curve slope of the wing leads to:

$$\frac{(l_{CW} - h_{AC})}{C_{MGC}} \left(\frac{S_C}{S} \right) \cdot \frac{C_{L_{\alpha C}}}{C_{L_{\alpha W}}} - \frac{h_n}{C_{MGC}} \left(\frac{S_C}{S} \right) \cdot \frac{C_{L_{\alpha C}}}{C_{L_{\alpha W}}} + \frac{C_{m_{\alpha AC}}}{C_{L_{\alpha W}}} - \frac{h_{AC}}{C_{MGC}} - \frac{h_n}{C_{MGC}} = 0 \quad (iii)$$

Then, solve Equation (iii) for h_n to determine the stick-fixed neutral point as a fraction of the MGC:

$$\frac{h_n}{C_{MGC}} \left(\frac{S \cdot C_{L_{\alpha W}} + S_C \cdot C_{L_{\alpha C}}}{S \cdot C_{L_{\alpha W}}} \right) = \frac{(l_{CW} - h_{AC})}{C_{MGC}} \left(\frac{S_C}{S} \right) \cdot \frac{C_{L_{\alpha C}}}{C_{L_{\alpha W}}} + \frac{C_{m_{\alpha AC}}}{C_{L_{\alpha W}}} - \frac{h_{AC}}{C_{MGC}} \quad (iv)$$

Apply some simple algebraic aerobatics to yield:

$$\frac{h_n}{C_{MGC}} = \frac{\frac{(l_{CW} - h_{AC})}{C_{MGC}} S_C \cdot C_{L_{\alpha C}} + S \cdot \left(C_{m_{\alpha AC}} - \frac{h_{AC}}{C_{MGC}} C_{L_{\alpha W}} \right)}{S \cdot C_{L_{\alpha W}} + S_C \cdot C_{L_{\alpha C}}}$$

QED

EXAMPLE C2-2:

Determine the stick-fixed neutral point of the canard of [Example C2-1](#) (and Figure C2-3), using the same data presented in that example.

SOLUTION:

By plugging and chugging Equation (C2-4) we get:

$$\frac{h_n}{C_{MGC}} = \frac{\left(\frac{l_{CW} - h_{AC}}{C_{MGC}} S_C \cdot C_{L\alpha_C} + S \cdot \left(C_{m\alpha_{AC}} - \frac{h_{AC}}{C_{MGC}} C_{L\alpha_W} \right) \right)}{S \cdot C_{L\alpha_W} + S_C \cdot C_{L\alpha_C}}$$

$$= \frac{\frac{(8.25 - 0.5)}{2.0} 6 \times 4.247 + 40 \left(0 - \frac{0.5}{2.0} 5.012 \right)}{(40 \times 5.012 + 6 \times 4.247)} = 0.2152$$

This places the stick-fixed neutral point some $0.2152 \times 2.0 \text{ ft} = 0.430 \text{ ft}$ ahead of the leading edge of the MGC. Note that if $h_n < 0$, then the neutral point is aft of (to the right of the LE in Figure C2-4).

C2.1.4 Sizing the Canard based on Requirements for the Trimmability

One of the most important tasks in canard design is the sizing of the canard itself. This involves selecting an airfoil for it and determining a suitable geometry (span, chord, and tail arm) and AOI that allows the airplane can be trimmed at some desired airspeed, typically cruising speed, with the elevator in trail (i.e. $\delta_e = 0^\circ$). To make this possible, we have to resort to the longitudinal stability theory derived in Equations (C2-1), (C2-2), and (C2-3). This is done below. Note that the sizing method should also be used while considering other conditions; for instance balked landing at forward CG. Then the tail geometry that satisfies all the flight conditions considered should be selected.

Figure C2-6 shows a standard C_m versus α curve, here representing a canard configuration aircraft. Effectively, it is a “cleaner” version of Figure C2-5. If the canard airfoil is symmetrical and, assuming neutral elevator deflection, the curve tends to be in a location below the horizontal axis, as indicated by the dashed curve. This was illustrated in [Example C2-1](#).

In order to trim the configuration at some desired AOA (denoted by α_{trim}) and given a longitudinal stability derivative, $C_{m\alpha}$, we want to size the canard so it generates enough lift to shift the pitching moment curve to the point C_{m0} , allowing it to be trimmed at a positive AOA. This, as we recall from [Section 11.2.1, Fundamentals of Static Longitudinal Stability](#), is necessary so the airplane can be trimmed at an AOA that results in a lift force vector that points in the opposite direction from the weight vector. It is a fundamental requirement for static stability.

To solve the issue with the low sitting C_m curve, we have to look at Equation (C2-2), which when combined with the elevator contribution can be written in the form shown below:

$$C_{m0} + C_{m\delta_e} \cdot \delta_e = C_{m0_{AC}} - \frac{C_{m\alpha_W}}{C_{MGC}} + \frac{S_C \cdot l_C}{C_{MGC} \cdot S} \cdot C_{L\alpha_C} + C_{m\delta_e} \cdot \delta_e \quad (\text{C2-5})$$

The problem is complicated by the fact that playing around with the variables may change the slope of the pitching moment curve as well. This is given by Equation (C2-3), repeated below:

$$C_{m\alpha} = C_{m\alpha_{AC}} + \frac{S_C \cdot l_C}{C_{MGC} \cdot S} \cdot C_{L\alpha_C} - \frac{(h_{AC} + h)}{C_{MGC}} C_{L\alpha_W} \quad (\text{C2-3})$$

The possible solution approaches are listed below:

(1) $C_{m_{0AC}}$ = Longitudinal stability contribution of components other than the wing. This means fuselage, nacelles, landing gear, and others. This contribution is not easily estimated unless the designer knows the geometry well in advance. It may well place the C_{m_0} lower or higher and, thus, it is necessary to estimate this contribution before the canard is sized. However, while the contribution may help, it should not be considered a possible solution.

(2) $C_{m_{ow}} = C_{L_{ow}} (h_{AC} + h)$ = Wing pitching moment due to wing airfoil camber. Due to the location of the CG forward of the aerodynamic center and the negative sign in front of the ratio in Equation (C2-3), this can only increase C_{m_0} if a reflexed airfoil (i.e. one whose camber is negative) is featured. This does not help with the sizing of the canard, although some remedy is to be had by selecting a main wing airfoil that does not have a large positive camber (of course as long as the lift capability of the aircraft is not compromised).

(3) $V_C = \frac{S_C \cdot l_C}{S \cdot C_{MGC}}$ = Canard volume. There are a number of options provided here, although these demand a cambered airfoil or an AOI greater than zero to be used in the canard design (as this results in a $C_{L_{oc}} > 0$). This way, the designer can increase the canard arm (l_C) or planform area (S_C). Playing around with the product $S \cdot C_{MGC}$ is also possible, albeit harder, as this will affect the total lift of the aircraft.

(4) $C_{L_{oc}}$ = Canard lift coefficient at zero AOA. This gives the designer two additional tricks up the sleeve; airfoil camber and AOI. Recall that this is the lift coefficient of the canard at zero AOA and this contribution can be adjusted using a combination of the zero-AOA lift of the airfoil and the canard's AOI.

(5) $C_{m_{\delta_e}} \cdot \delta_e$ is the contribution of the elevator deflection. The designer should use this parameter dependent on a particular flight condition. For instance, for balked landing case this could be $\delta_e = +12^\circ$ (TED). When evaluating the canard size for the design mission weight and CG-location, then the elevator should be in trail (i.e. $\delta_e = 0$). This contribution is used to accommodate off-design flight and weight. Remember that no flight condition should lead to the pilot running out of elevator deflection.

(6) $C_{L_{\alpha C}}$ = Canard lift curve slope. By increasing the lift curve slope of the canard (i.e. increasing its AR), the designer can reduce stability (destabilize the aircraft), i.e. make $C_{m\alpha}$ shallower. This, in turn, requires less C_{m_0} to be established. For this reason, the AR becomes an important design parameter.

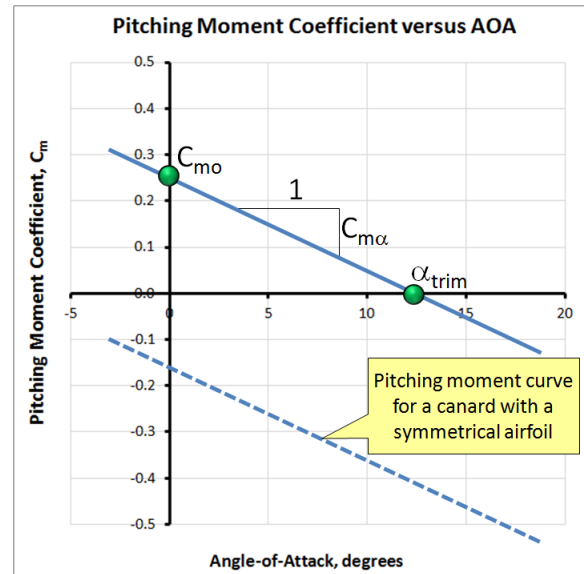


Figure C2-6: A pitching moment for a stable canard with a symmetrical canard airfoil, mounted at a zero AOI, as a function of AOA

EXAMPLE C2-3:

Assume the canard of Example C2-1 (and Figure C2-3) is to be operated at a cruise condition that calls for a trim AOA of 5° with the CG located at the previous position ($h = 0.783$ ft). Evaluate the following:

(a) The canard arm, l_C , given the airplanes fixed initial planform area of 6 ft^2 and,

(b) The planform area, S_C , given the airplanes fixed initial canard arm (l_{CW}) of 8.25 ft that will allow for this, by assuming airfoils that have a $C_{L_{0C}}$ of 0.1, 0.2, 0.3, and 0.4.

Note that these factors will change the $C_{m\alpha}$ as well, so include this effect as well.

SOLUTION:

This problem can be tackled by plotting the complete C_m curves while holding all but the cited variables constant.

(a) First consider how changing the canard arm will affect the pitching moment curve, as the initial planform area of 6 ft² is held constant. The resulting trends are shown in Figure C2-7. It shows that, for canard airfoils that result in $C_{L_{0C}}$ ranging from 0.1 to 0.4, the required canard arm, l_C , ranges from about 9 ft to 14.75 ft. A sample calculation at $\alpha = 5^\circ$ for $l_C = 2 \text{ ft}$ and $C_{L_{0C}} = 0.4$ is shown below:

$$C_{m_o} = C_{m_{0AC}} - \frac{C_{m_{ow}}}{C_{MGC}} + \frac{S_C \cdot l_C}{C_{MGC} \cdot S} \cdot C_{L_{0C}} = 0 - \frac{0.513}{2.0} + \frac{6 \times 2}{2.0 \times 40} (0.4) = -0.1966$$

$$C_{m_\alpha} = C_{m_{\alpha AC}} + \frac{S_C \cdot l_C}{C_{MGC} \cdot S} \cdot C_{L_{\alpha C}} - \frac{(h_{AC} + h)}{C_{MGC}} C_{L_{\alpha W}}$$

$$= 0 + \frac{6 \times 2}{2.0 \times 40} (4.52) - \frac{(0.5 + 0.783)}{2.0} (5.15) = -2.626$$

$$\Rightarrow C_m = C_{m_o} + C_{m_\alpha} \alpha = -0.1966 - 2.626 \times 5 \times (\pi/180) = -0.4258$$

(b) Then, the effect of changing the canard planform area while holding the initial canard arm of 8.25 ft constant is shown in Figure C2-8. It shows for the same canard airfoils that the required canard planform area, S_C , ranges from about 9 ft to 14.75 ft. It indicates that for the given arm of 8.25 ft, a $C_{L_{0C}}$ in excess of 0.2 is required. A sample calculation at $\alpha = 5^\circ$ for $l_C = 2 \text{ ft}$ and $C_{L_{0C}} = 0.4$ is shown below:

$$C_{m_o} = C_{m_{0AC}} - \frac{C_{m_{ow}}}{C_{MGC}} + \frac{S_C \cdot l_C}{C_{MGC} \cdot S} \cdot C_{L_{0C}} = 0 - \frac{0.513}{2.0} + \frac{6 \times 2}{2.0 \times 40} (0.4) = -0.1966$$

$$C_{m_\alpha} = C_{m_{\alpha AC}} + \frac{S_C \cdot l_C}{C_{MGC} \cdot S} \cdot C_{L_{\alpha C}} - \frac{(h_{AC} + h)}{C_{MGC}} C_{L_{\alpha W}}$$

$$= 0 + \frac{6 \times 2}{2.0 \times 40} (4.52) - \frac{(0.5 + 0.783)}{2.0} (5.15) = -2.626$$

$$\Rightarrow C_m = C_{m_o} + C_{m_\alpha} \alpha = -0.1966 - 2.626 \times 5 \times (\pi/180) = -0.4258$$

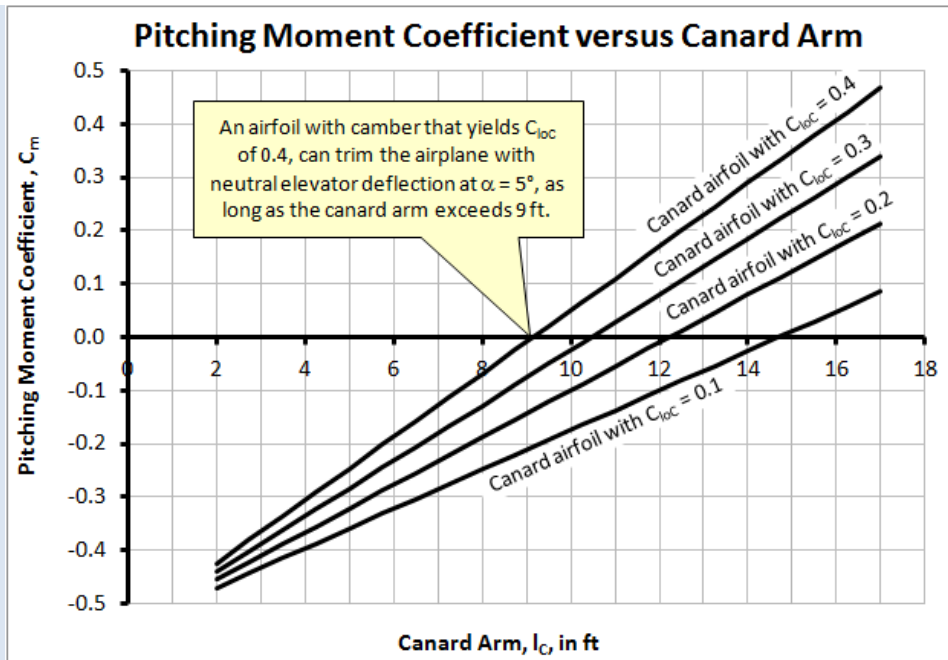


Figure C2-7: The pitching moment coefficient plotted in terms of the canard arm, constant $S_C = 6 \text{ ft}^2$, and considering four airfoil options. This reveals that the example aircraft will need a highly cambered airfoil if the goal is to keep the length of the fuselage down. Note that $SM = 0.10$ and $\alpha = 5^\circ$.

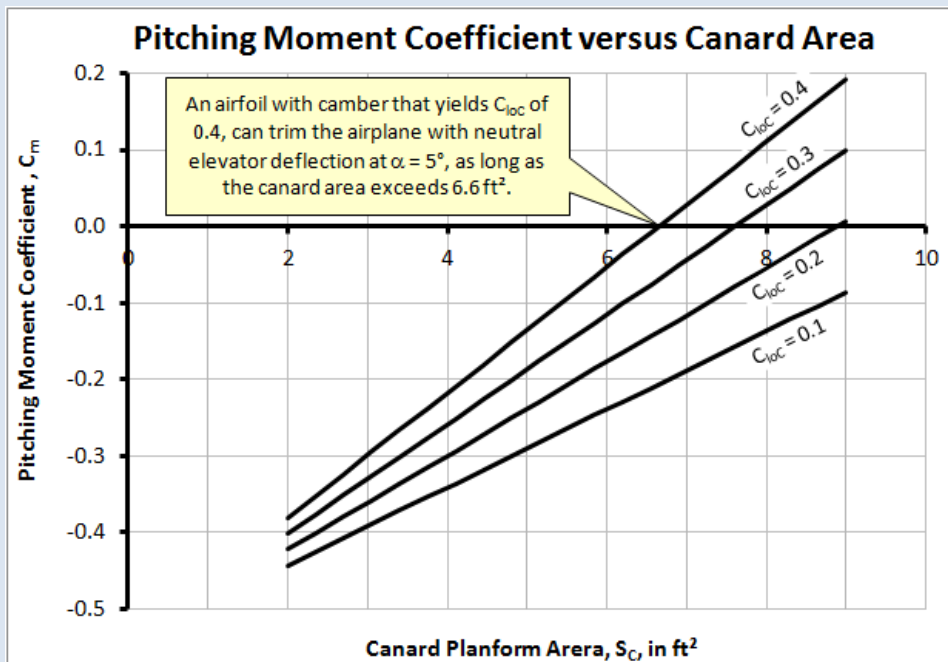


Figure C2-8: The pitching moment coefficient plotted in terms of the canard planform area, constant $l_C = 8.25 \text{ ft}$, and considering four airfoil options. This reveals that the example aircraft will also need a highly cambered airfoil to keep the size of the canard down. Note that $SM = 0.10$ and $\alpha = 5^\circ$.

C2.1.5 Achieving Stall Proofing in a Canard

Designing stall-proofing is a challenge and must be done with utmost care. It can be solved using a combination of specially selected airfoils, AR, AOI, and even sweep and Taper Ratio. Stall proofing requires the stall AOA of the canard to be lower than that of the wing. Following are important effects to keep in mind:

(1) The canard airfoil should have gentle stall characteristics to avoid too abrupt a nose drop. This can be achieved using a highly cambered airfoil. The preceding discussion shows that highly cambered airfoils have a side-benefit in its higher zero AOA lift coefficient, required to allow the vehicle to be trimmed at the mission design airspeed with zero elevator deflection.

(2) The magnitude of the AR affects the AOA of stall. A large AR reduces the AOA of stall, while a small AR does the opposite. Another benefit of the high AR is a steeper lift curve slope that produces higher lift at a given AOA. This allows for a smaller canard than otherwise and an installation at a lower AOI.

(3) High AR results in a short chord with a low Re . This may result in undesirable characteristics at low speeds, such as the formation of a laminar separation bubble (or a spanwise vortex) along the surface that may yield detrimental stall characteristics. High AR canards are also sensitive to surface contamination; for a small chorded airfoil, a squished bug is akin to a mountain on a plain. Even precipitation will affect its characteristics. Both the VariEze and LongEz have a reputation of nose-drop when flying in precipitation, as pointed out in [Section C2.1.1, Pros and Cons of the Canard Configuration](#). Additionally, using experimental data, Yip² demonstrates that the lift curve of the canard is greatly affected by Reynolds numbers.

(4) AOI can be used to further fine tune the AOA at which the canard begins to stall. This is demonstrated in Reference 2.

(5) Sweepback will modify the lift curve slope in a similar manner as a reduction in AR. However, it will also tip load the canard and lower its stall AOA. A similar effect is achieved with a high taper. Both are possible tools to control the stall (and lift) characteristics, although the designer should keep in mind that most of the successful canard aircraft have straight constant chord canards.

C2.1.6 Rutan VariEze in the Wind Tunnel

In 1985 NASA released Technical Paper 23822, which presented the results of a wind-tunnel test conducted on a full scale Rutan VariEze. The airplane was tested in the now leveled 30x60 foot Langley Full Scale Tunnel (LFST) in Langley, Virginia (see Figure C2-9). The paper provides the designer with a wealth of knowledge on what actually takes place on a canard as its AOA increases. If you are designing a new canard you would be well advised to familiarize yourself with its content. The paper reveals the secret behind the stall characteristics of canards.

Consider Figure C2-10, which shows the lift curve for the VariEze. The left graph shows the lift curve for the complete airplane and the canard, while the right one shows the lift of the canard only. Both lift curves are based on the wing area of the aircraft, which is 53.6 ft². This explains why the lift curve for the canard in the left graph appears so much lower than that of the main wing. This is remedied in the right graph, which effectively zooms in on the lift curve for the canard only.

The left graph of Figure C2-10 shows the main wing stalls at $\alpha = 23.5^\circ$. However, the lift curve for the canard in the right graph shows its $C_{L\alpha}$ is sharply reduced at $\alpha = 13.5^\circ$. Adhering to NACA's definition of stall as the first peak in the lift curve, the canard is technically not stalled (even though it is called so in the reference). Rather it eventually stalls at $\alpha = 23.5^\circ$, the same as the wing! The change in slope is most likely caused by a sudden flow separation along the trailing edge of the highly cambered airfoil, which operates at a relatively low Reynolds Number. It is this behavior of the GU25-5(11)8 airfoil used for the canard that has a lot to do with the gentle stall characteristics of the airplane. A comparatively abrupt stall of the typical airfoil would likely cause the airplane to drop its nose far more aggressively. Later models of the VariEze were equipped with a "cuff" or a leading edge extension on the outboard portion of the swept aft main wings, installed to improve the airplane's roll stability at stall.

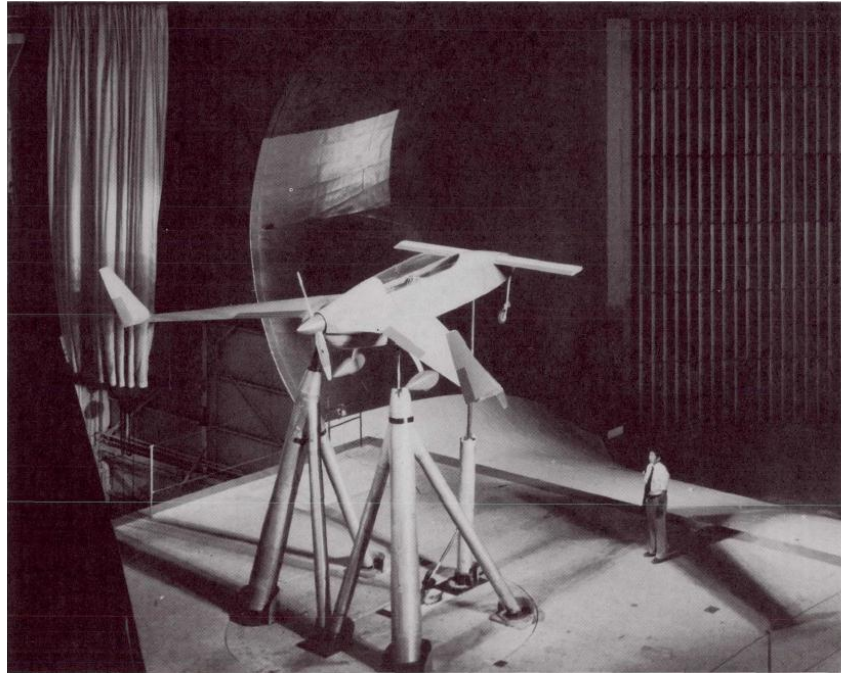


Figure C2-9: An image from Reference 2, showing the Rutan VariEze mounted in the wind tunnel at the LFST.

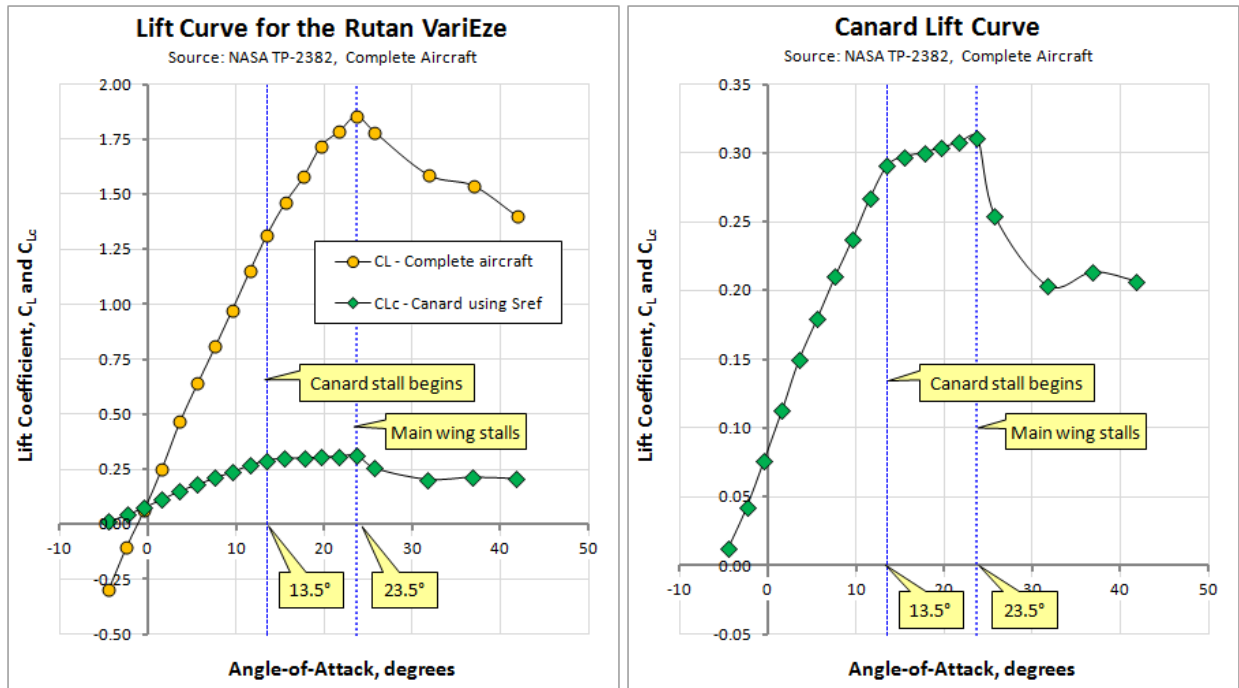


Figure C2-10: The lift curves for the entire aircraft and the canard. The right graph shows the lift curve of the canard in detail. (Reproduced from Reference 2)

Now consider Figure C2-11. The pitching moment is plotted as a function of the AOA with and without a wing cuff. The dashed vertical lines denotes $\alpha = 13.5^\circ$, which is where the canard's lift curve slope changes suddenly, and $\alpha = 23.5^\circ$, where the main wing stalls. The change in the slope of the pitching moment curve ($C_{m\alpha}$) becomes even more negative at the former AOA, due to the reduced "growth" in the stabilizing force of the canard. This helps to force the nose down, preventing the aircraft's main wing from stalling. Since the slope of the canard's lift curve is

reduced, rather than becoming negative for the AOA range from 13.5° to 23.5°, the result is a gentle nose drop, the reason for the airplane’s renowned stall recovery characteristics.

The designer of canards should be aware of these effects, and carefully consider airfoils with aerodynamic properties similar to that of the GU25-5(11)8 airfoil used for the VariEze. The relatively low operational Reynolds Number of canard airfoils must also be considered, as this will influence the stall characteristics of the canard.

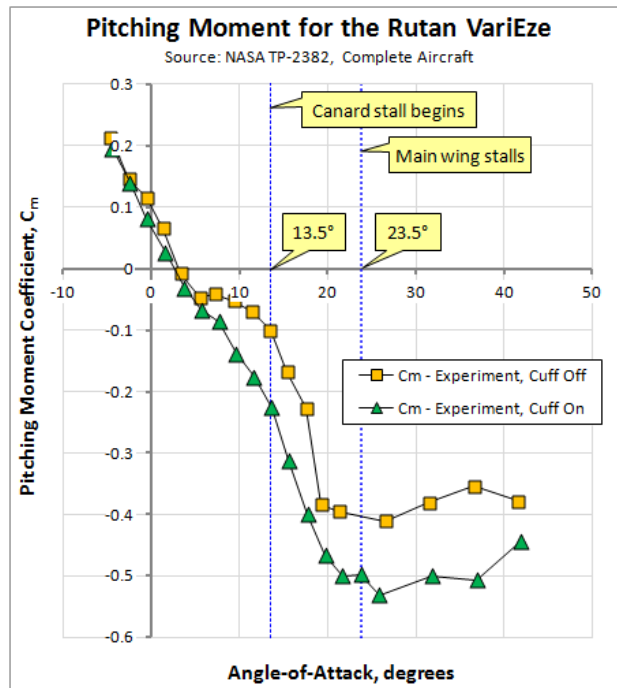


Figure C2-11: The pitching moment for the Rutan VariEze with and without leading edge droops (cuffs). (Reproduced from Reference 2)

C2.1.7 Configuration Comparison

A common claim among laypeople holds that the canard configuration is superior to the tail-aft configuration. They point at the Rutan LongEz, a truly efficient aircraft, and compare it to other less efficient airplanes familiar to them, such as a Cessna 152 or Piper PA-38 Tomahawk. The astute ask then, if this is true, then why are there not more canard configurations around? For instance, why aren’t most sailplanes of a canard configuration?

The fact is that any such comparison must be done on a level playing field. The LongEz is not more efficient than the 152 or PA-38 because it is a canard, but rather because of the mission of the airplane. The LongEz is not a primary trainer like the other two, but a touring aircraft. In fact, its take-off and landing characteristics (high speed) make it all but unfit as a primary trainer, not to mention it is unsuitable for gravel runways. Additionally, there is difference in wing area (LongEz has 82 ft², Cessna 152 has 160 ft² and PA-38 has 125 ft²) and gross weight (LongEz is 1325 lb_f, Cessna 152 and PA-38 are 1670 lb_f), although power is similar (LongEz has 115 BHP, Cessna 152 has 110 BHP and PA-38 has 112 BHP). The comparison is thus unfair and without a foundation.

This section is intended to inspire the designer to conduct realistic “apples-to-apples” comparison on the candidate configurations. One method is to compare a basic tail-aft configuration (Configuration A) to a basic canard configuration (Configuration B), for instance using potential flow theory. This approach is implemented below. Both configurations (see Figure C2-12) have the same wing and stabilizing surface geometry (including elevators), the only difference is that Configuration A has the HT aft of the wing and B ahead of the wing. Both tail arms are equally long (8.25 ft). For simplicity there is no provision made for a fuselage. Both have the CG at position such the Static Margin (SM) is 0.1 and both are assumed to weigh 400 lb_f. The wing airfoil is NACA 4415 and the stabilizing surface has a symmetrical airfoil, which as shown earlier is problematic for a canard configuration.

Here, consider the following scenario. If both configurations are trimmed at 100 KCAS at S-L, the following questions are of interest:

- (1) What is the difference in AOA and elevator angle to trim (δ_e) at a given airspeed?
- (2) Which configuration generates higher lift-induced drag at that airspeed?

The answer to these questions is key in understanding the difference between the two configurations. And this calls for more powerful tools than classical analysis – here potential flow modeling will be used. This improves accuracy as it subjects both configurations to a reasonably accurate distortion of the flow field and this is fundamental to their capabilities.

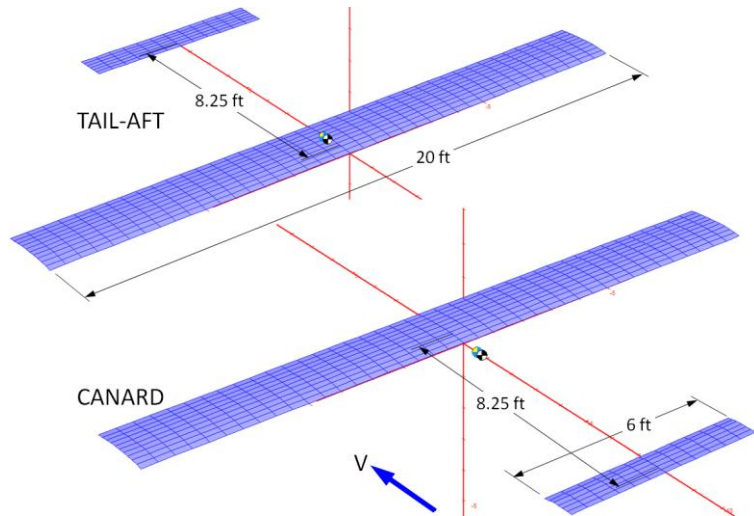


Figure C2-12: The two VL models. The conventional configuration is to the left and canard to the right.

The code used here is a commercially available code called SURFACES and it uses the Vortex-Lattice Method (VLM). The reader can download free VLM solvers like Mark Drela’s AVL and perform a similar analysis. However, all talk of potential flow theory should spur questions of validation: How accurate is it when compared to experiment? To address this question a detailed model of the VariEze was prepared, using the geometry presented in Reference 2. This is addressed in Figure C2-13, which shows a VLM model used to evaluate prediction potential and how its lift and longitudinal stability predictions compare to that of the experiment. Note that deviations from the straight line predictions of the VLM code are due to various viscous effects not being modeled by such programs. It can be seen that at least for this model, there is a good agreement between theory and experiment in the linear region.

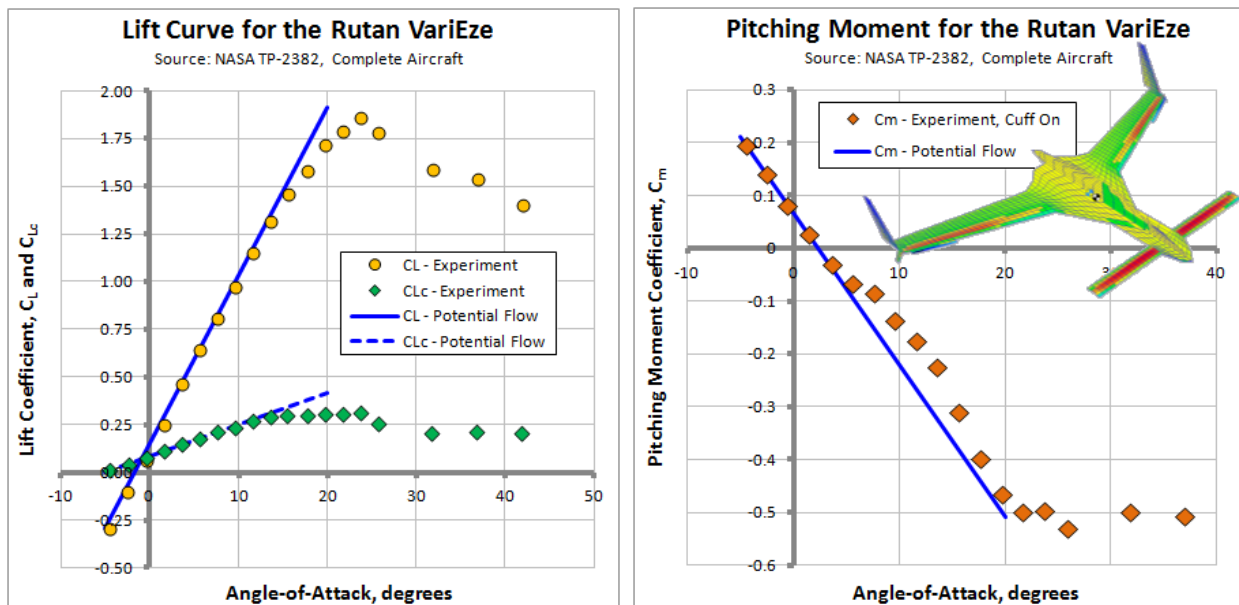


Figure C2-13: Comparing lift and pitching moment of a validation model to experiment.

In order to keep the complexity of the models to a minimum, both wings are constant chord and straight (see Figure C2-12). The two models do not feature vertical stabilizers, as the purpose is only to compare their lifting and

longitudinal stability properties. Additionally, since the purpose of this appendix is to qualitatively compare properties rather than demonstrate how these were determined (which would require considerably larger space) these are omitted. Instead, the basic geometry is provided for the interested reader who may want to construct own models for comparison.

Differences in Lift, Drag, and Longitudinal Stability

The properties of the two configurations in Figure C2-12 are shown in Table C2-1 and Figure C2-14 and Figure C2-15. Recall that both configurations weigh 400 lb_f and are trimmed at 100 KCAS at S-L. The table reveals a number of very interesting differences.

- (1) The lift-induced drag of the two configurations was predicted using Prandtl-Betz integration on the Trefftz plane. The results indicate this drag is less for the canard configuration than the tail-aft configuration over a range of airspeeds between 40 and 85 KCAS, but actually greater at higher airspeeds. The variation ranged from 14 drag counts at low airspeeds to -10 at high airspeeds. Naturally, these are theoretical predictions and they may be off. However, they highlight that the efficiency of a particular configuration is indeed mission related.
- (2) The canard requires lower AOA to generate the same lift as the tail-aft configuration (-1.09° versus -0.39°) at the 100 KCAS airspeed (see Table C2-1). This means that the canard is also at a lower AOA and calls for a larger elevator deflection than otherwise.
- (3) Note the position of the neutral points shown in Table C2-1. These will both move forward with the introduction of a fuselage.
- (4) The elevator deflection required to balance the canard configuration is substantially greater than that of the tail-aft configuration, or 10.99° versus 1.24°. Recall that the canard is the subject of Examples C2-1 through C2-3. The tail conventional configuration is located in the downwash from the main wing, so its angle of attack is higher than indicated by the incidence angle. Consequently, it requires less elevator deflection to balance the airplane. The canard, on the other hand, is in a modest upwash. It has to make up for the deficiency by the extra deflection. Again, this highlights why highly cambered airfoils have to be considered for the canard.

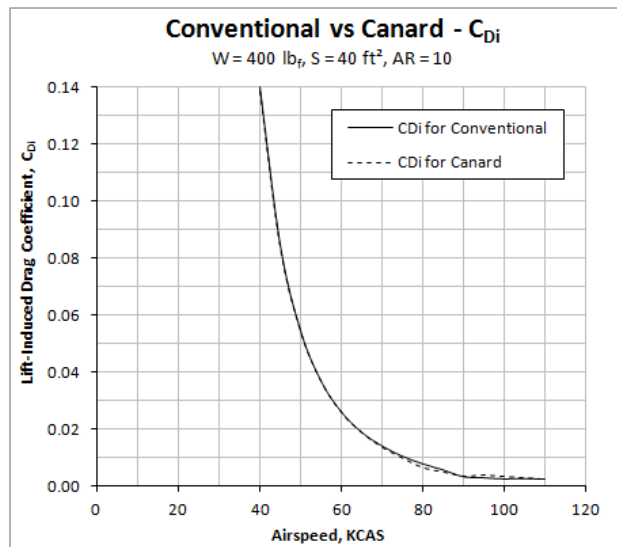


Figure C2-14: Comparing lift-induced drag of the conventional and canard configurations.

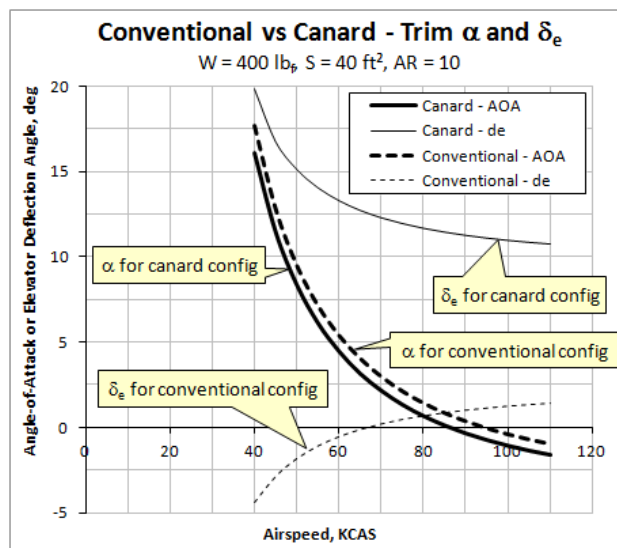


Figure C2-15: Comparing AOA and elevator deflection required to trim the conventional and canard configurations at the given airspeed.

Table C2-1: Properties of the Two Models

Property Description	Conventional	Canard
Wing span	20 ft	20 ft
Wing chord, root	2 ft	2 ft
Wing chord, tip	2 ft	2 ft
Wing Aspect Ratio	10	10
Wing airfoil	NACA 4415	NACA 4415
Angle of incidence	0°	0°
HT span	6 ft	6 ft
HT chord, root	1 ft	1 ft
HT chord, tip	1 ft	1 ft
HT Aspect Ratio	6	6
HT airfoil	Symmetrical	Symmetrical
Tail arm	8.25 ft	-8.25 ft
Elevator chord fraction	33%	33%
Angle of incidence	0°	0°
Weight	400 lb _f	400 lb _f
CG-location at 10% static margin	1.239 ft	-0.783 ft
Airspeed (100 KCAS)	168.8 ft/s	168.8 ft/s
Neutral point – Absolute	1.239 ft	-0.583 ft
Neutral point - %MGC	61.95%	-29.15%
AOA to trim at 100 KCAS at S-L	-0.39°	-1.09°
δ_e to trim at 100 KCAS at S-L	1.24° (TED)	10.99° (TED)
Lift coefficient	0.295	0.295
Lift-induced drag coefficient	0.00236	0.00324

Differences in Distribution of Section Lift Coefficients on Wing and Stabilizer

Figure C2-16 shows the distribution of the lift on the main wings of each configuration. Trimmed at 100 KCAS, the maximum section lift coefficient on the conventional configuration is 0.331 in the plane of symmetry (typical for a constant chord or “Hershey bar” wing), and 0.333 for the canard. Note the drop in section lift coefficients over the middle of the main wing of the canard configuration, caused by the downwash from the canard. For this reason, the AOA of the canard configuration is always (slightly) higher than if this effect was absent.

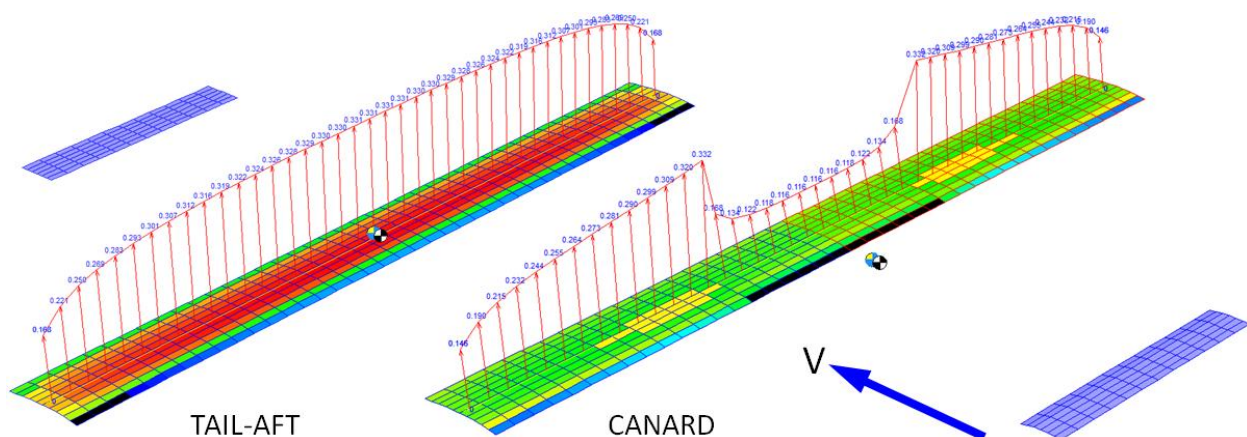


Figure C2-16: Distribution of section lift coefficients on the wing.

The distribution of the section lift coefficients is also of great importance. The maximum section lift coefficient on the HT is -0.041 and +0.539 on the canard at the same condition (trimmed at 100 KCAS). This shows that the canard must be loaded much more severely in order to generate a balancing force than the HT. Table C2-2 shows the difference in lift generated by the wing and the stabilizing surfaces. Note that the lift coefficient for the HT and canard are based on the reference wing area.

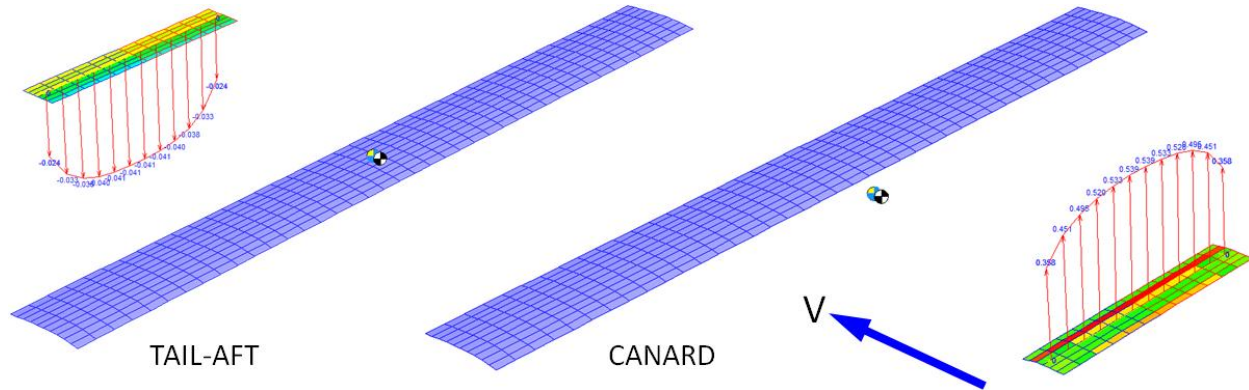


Figure C2-17: Distribution of section lift coefficients on the stabilizing surfaces.

Table C2-2: Lift Generated by the Two Models

Property Description	Conventional	Canard
C_L generated by main wing	0.3009	0.2228
C_L generated by horizontal tail	-0.0055	0.0726
Lift coefficient, total	0.2954	0.2954

The analysis shows that the main wing of the conventional configuration must generate lift in excess of what is required for level flight. This is caused by the horizontal tail having to generate balancing lift that points downward and the main wing must carry this force in addition to the weight. The magnitude of this additional lift increases as the CG moves forward. Generally, as a rule-of-thumb, the larger the HT load the higher is the AOA required for the configuration and, therefore, the higher the lift-induced drag. The opposite holds for the canard configuration. The main wing of the canard configuration generates less lift than the conventional configuration and the magnitude of the balancing force generated by the canard is larger than that of the HT and it points in the opposite direction and, therefore, contributes indeed to the total lift.

The bottom line is that the designer of efficient airplanes should attempt a careful study of proposed configurations and the mission design conditions in order to justify as particular geometry and configuration. While it is possible that one configuration leads to a more efficient aircraft than another one, this does not constitute a rule-of-thumb.

REFERENCES

¹ Rutan Aircraft Factory, *Long-EZ – Owner’s Manual*, 2nd Ed., October 1981.

² NASA TP-2382, *Wind-Tunnel Investigation of a Full-Scale Canard-Configured General Aviation Airplane*, Yip, Long P., 1985.